Germinal center reutilization by newly activated B cells

Tanja A. Schwickert,[1] Boris Alabyev,[3] Tim Manser,[4] and Michel C. Nussenzweig[1,2]

[1]Laboratory of Molecular Immunology and [2]Howard Hughes Medical Institute, The Rockefeller University, New York, NY 10065
[3]Department of Microbiology and Immunology, Thomas Jefferson University, Philadelphia, PA 19107
[4]Nanogen Inc., Bothell, WA 98021

Germinal centers (GCs) are specialized structures in which B lymphocytes undergo clonal expansion, class switch recombination, somatic hypermutation, and affinity maturation. Although these structures were previously thought to contain a limited number of isolated B cell clones, recent in vivo imaging studies revealed that they are in fact dynamic and appear to be open to their environment. We demonstrate that B cells can colonize heterologous GCs. Invasion of primary GCs after subsequent immunization is most efficient when T cell help is shared by the two immune responses; however, it also occurs when the immune responses are entirely unrelated. We conclude that GCs are dynamic anatomical structures that can be reutilized by newly activated B cells during immune responses.

CORRESPONDENCE
Michel C. Nussenzweig:
nussen@rockefeller.edu

Abbreviations used: Ars, arsonate; CGG, chicken gamma globulin; FDC, follicular DC; GC, germinal center; NP, 4-Hydroxy-3-nitrophenol; PC, phosphorylcholine; RNP, ribonuclear protein.

Germinal centers (GCs) were first described by histologists in 1884 and named as such because they were thought to be the site of lymphoid cell development. In the last century, we learned that GCs are actually sites of B cell clonal expansion and diversification (Berek et al., 1991; Jacob et al., 1991; MacLennan, 1994). These structures are formed during immune responses and remain for 20–100 d after immunization (Liu et al., 1991; Bachmann et al., 1996). During this period, they continually produce expanded clones of memory B cells and plasma cells that are related by somatic hypermutation (Jacob et al., 1991; Liu et al., 1991).

After antigen capture, B cells migrate to the interface between the T and B cell zones in lymphoid organs, where they cluster with antigen-specific T cells and DCs and begin dividing (Ansel et al., 1999; Okada and Cyster, 2006; Coffey et al., 2009). Subsequently, one to five clones of dividing B cells migrate into the B cell follicle and form antigen-specific GCs, which also contain follicular DCs (FDCs), tingible body macrophages, specialized follicular helper T cells, and conventional DCs (Kroese et al., 1987; Jacob et al., 1991; Liu et al., 1991; Küppers et al., 1993). FDCs differentiate from existing mesenchymal cells in the B cell follicle and express receptors for immune complexes, which facilitate the capture and prolonged display of antigen which is believed to contribute to the selection of B cells bearing mutated high-affinity receptors.

Once a GC is established in the B cell follicle it develops dark and light zones, which were traditionally thought to be the sites of clonal expansion and selection, respectively. However, intravital imaging revealed that GC B cells move between the light and dark zone compartments in a manner that makes this simple model improbable (Allen et al., 2007; Hauser et al., 2007; Schwickert et al., 2007; Figge et al., 2008). In addition, GCs were found to be open structures that include naive follicular B cells, which are frequent visitors to the light zones (Allen et al., 2007; Schwickert et al., 2007). These B cells, which do not appear to actively participate in the reaction, make contact with FDCs, suggesting that all such B cells may deliver antigen to GCs as well as scan for cognate antigen (Schwickert et al., 2007; Suzuki et al., 2009). Consistent with the idea that GCs remain open, B cells bearing high-affinity receptors specific for the initial immunogen are recruited to an ongoing GC reaction, which suggests a mechanism whereby cognate antigen-specific B cells that were not

The Rockefeller University Press $30.00
J. Exp. Med. Vol. 206 No. 13 2907-2914
www.jem.org/cgi/doi/10.1084/jem.20091225

The Journal of Experimental Medicine

initially involved could also join in an ongoing immune response (Schwickert et al., 2007). However, the possibility that GCs might also be co-opted during immune responses to unrelated antigens was not examined.

In this paper, we show that preexisting GCs are reutilized during heterologous immune responses. Sequential immunization with two different haptens produced GCs with mixed hapten-specific B cell populations, which demonstrates the plasticity of the GC microenvironment. We conclude that GCs are not limited to one time use. On the contrary, they are open to reutilization during immune responses to unrelated antigens.

RESULTS AND DISCUSSION

B cells use preexisting GCs

To examine the relationship between B cells that respond to two different antigens in vivo, we initially made use of previously characterized mice that carry targeted Ig genes specific for either 4-hydroxy-3-nitrophenol (NP) or arsonate (Ars; Liu et al., 2007; Shih et al., 2002). Mutant mice carrying the NP (B1-8^{hi})- or Ars (HKI65/Vk10)-specific B cells were maintained on a B6-CD45.2 background. Those with the NP-specific antigen receptors also carried a transgene encoding GFP (Schaefer et al., 2001) to facilitate cell tracking in B6-CD45.1 hosts (Fig. 1 a).

In adoptive transfer experiments, 8 d after immunization with Ars–keyhole limpet hemocyanin (KLH) in alum, large GCs containing B cells specific for Ars were present (Fig. 1 a, right). To determine whether heterologous B cells would enter and participate in an ongoing GC reaction, mice with Ars-specific GCs received NP-specific B cells and were boosted with NP-KLH (Fig. 1 a). 6 d after the boost, the composition of the GCs was assessed by immunohistology (Fig. 1 b). In theory, this protocol could have produced three outcomes: GCs containing either Ars- or NP-specific B cells, or a mixture of both (Fig. 1 c). Most (73%) GCs contained both NP- and Ars-specific B cells (60 out of 82 GCs; Fig. 1, b [right] and c). Only 24% of the GCs were NP restricted, and these may have contained endogenous KLH-specific B cells which were not visualized (20 out of 82 GCs; Fig. 1 c). A very high efficiency of invasion of preexisting GCs is demonstrated by the fact that only a minor fraction (2%) of all GCs is Ars-restricted (2 out of 82 GCs; Fig. 1 c). In contrast, control mice that received the heterologous B cell transfer but were primed and boosted with either Ars-KLH or NP-KLH exhibited GCs containing only Ars- or NP-specific B cells, respectively (49 out of 49 GCs or 33 out of 33 GCs, respectively; Fig. 1, b [middle and left] and c).

The experiments reported in the previous paragraphs were performed with B cells carrying knockin antigen receptors. To determine whether B cells invade GCs specific for heterologous antigens under physiological conditions, an experiment was performed in which we immunized and boosted wild-type mice and examined GC B cells by laser microdissection and DNA sequencing. C57BL/6 mice immunized with phosphorylcholine (PC; Rudikoff and Potter, 1980; Ruppert et al., 1980) or NP (Reth et al., 1978) develop canonical B cell immune responses dominated by specific anti-hapten IgH VDJs (VH186.2/JH2 for NP and S107/J_H1 for PC; Fig. S1 a). Genomic DNA isolated separately from three GC serial sections was used for gene amplification. Clonal expansion was demonstrated by the presence of related B cell clones in independent serial sections in the same GC (Fig. S1 a, bottom). In samples that were immunized and boosted with PC-KLH, we found expanded B cell clonal families with unique S107/J_H1 V(D)Js in the lymph nodes of four immunized mice. Expanded clones varied in size from 3–11 members, which were related by somatic hypermutation (Fig. S1 b). The same GCs also contained occasional B cells bearing the VH186.2/JH2 heavy chain; however, these cells were not clonally expanded, suggesting that they might have been unique B cells in transit through the GC. In contrast, mice immunized with PC-KLH followed by NP-KLH showed expanded clones of both B cells bearing unique S107/J_H1 and V_H186.2/J_H2 recombination in the same GC (Fig. S1, b and c; and Fig. S2). We conclude that sequential administration of two antigens that share the same carrier leads to efficient invasion of GCs by heterologous high-affinity B cells.

Studies in pathogen-free mice showed that GCs are rapidly induced by immunization and subsequently regress after 3–14 wk (Jacob et al., 1991; Liu et al., 1991; Bachmann et al., 1996). However, GCs appear to be constant features of secondary lymphoid tissues like human tonsils and Peyer's patches, which are continually exposed to antigens. Our experiments reconcile these two apparently conflicting observations by demonstrating that GCs can be reutilized during immune responses to heterologous antigens.

In addition to obviating the requirement of reconstructing the GC environment, the observation that existing GCs can be used by newly activated B cells is consistent with, and may provide a physiological context for, the fact that B cells that are nonspecifically stimulated by transgenic expression of LMP2A can be found in GCs in Peyer's patches (Casola et al., 2004). Accordingly, activated B cell entry into an ongoing GC may be a default option when the existing structure is available.

Kinetics of GC invasion

To further investigate B cell invasion of preexisting heterologous GCs, we examined the kinetics of this specific response. Allotype-marked Ars-specific B cells were transferred to B6-CD45.1 recipients 1 d before immunization with Ars-KLH in alum. Mice were boosted with NP-KLH 8 d after the initial immunization and received NP-specific B cells after one additional day (Fig. 2 a).

1 d after the NP-specific B cell transfer, when Ars-specific GCs were already established, the NP-specific B cells were distributed throughout the B cell follicle (Fig. 2 b, left). As early as 2 d after NP-specific B cell transfer, these cells were concentrated at the T-B interface. By day 4, they completely populated Ars-specific GCs (Fig. 2 b, middle and right, respectively).

B cells are activated by surface immunoglobulin cross-linking by soluble antigen or deposits of immune complexes

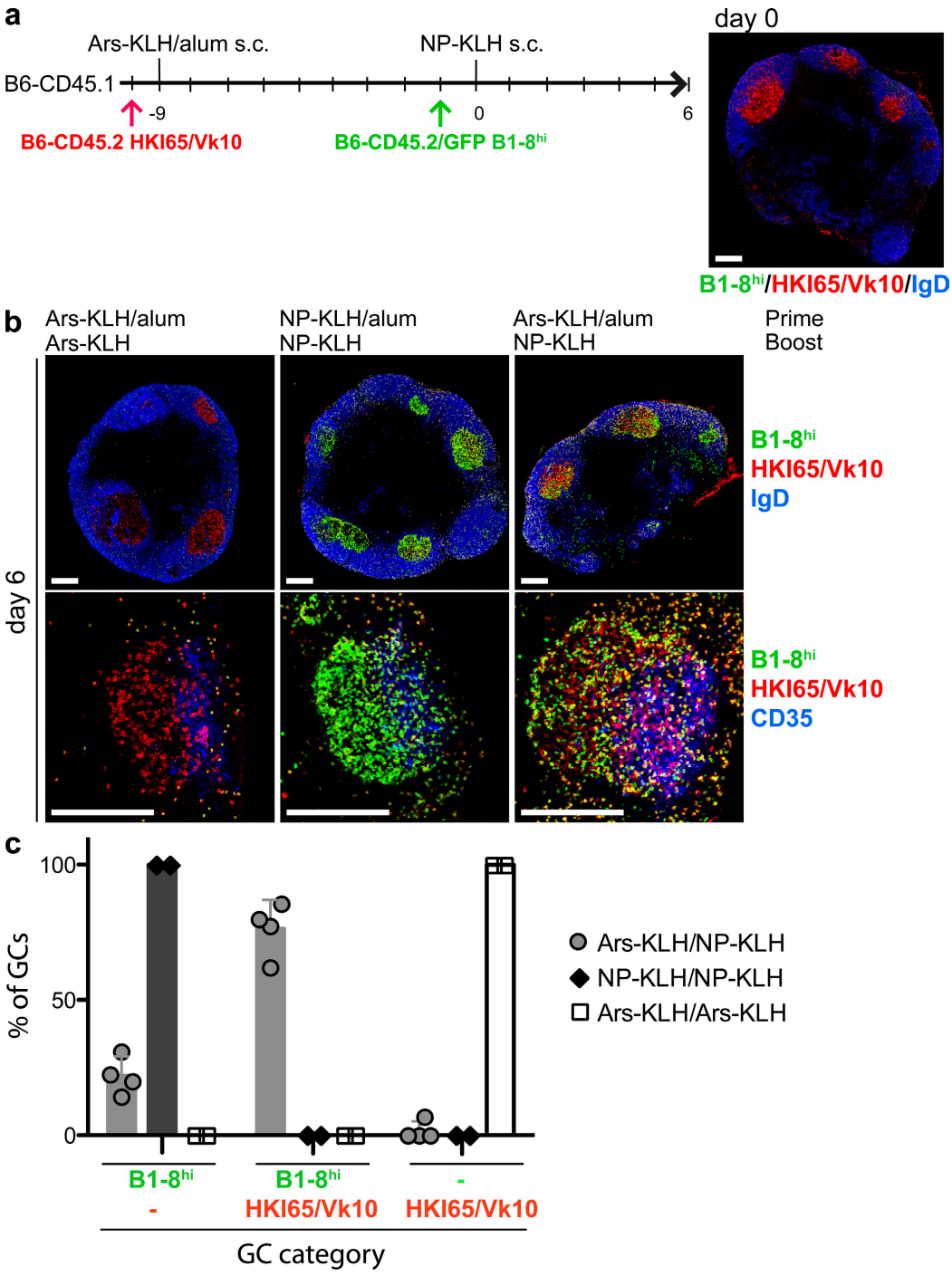

Figure 1. B cell invasion of established GCs. (a) Time line of immunization and B cell transfer. Ars-specific B cells (B6-CD45.2 HKI65/Vk10) were transferred 1 d before primary immunization (day −10) and NP-specific B cells (B6-CD45.2/GFP B1-8^{hi}) were transferred 1 d before boosting (day −1) into wild-type (B6-CD45.1) mice. Ars-specific GCs were detected in histological sections, 9 d after priming (day 0; right: B6-CD45.2/GFP B1-8^{hi} [green and red], B6-CD45.2 HKI65/Vk10 [red], IgD [blue]). (b) Representative histological sections of lymph nodes harvested 6 d after NP-KLH boost. Both transferred B cell populations (HKI65/Vk10 and B1-8^{hi}) are membrane stained by CD45.2 (red), whereas B1-8^{hi} B cells are additionally GFP^{+} (green; B1-8^{hi} appear yellow because of GFP/CD45.2 double staining). To visualize GCs within secondary follicles, mantle zone B cells were stained by IgD (blue, top) or FDCs were stained by CD35 (blue, bottom). The top row shows whole cross sections of popliteal lymph nodes, and the bottom row shows more magnified views of GCs. Priming and boosting antigens are indicated at the top. Bars, 200 µm. (c) Statistical analysis of data shown in b. GCs were categorized in three groups: GCs with only NP-specific B cells, with both NP- and Ars-specific B cells, or with only Ars-specific B cells. Each data point represents the percentage of GCs in one of the categories for each mouse. Error bars show the standard deviation. Two independent experiments were performed with a total of four mice (two mice per control).

on FDCs and subcapsulary sinus macrophages (Carrasco and Batista, 2007; Junt et al., 2007; Phan et al., 2007; Roozendaal et al., 2009). Once activated, B cells express CCR7, a chemokine receptor which facilitates the cells' migration to the interface between the T cell zone and the B cell follicle (Ansel et al., 1999; Okada et al., 2005). After receiving cognate T cell help, B cells begin to proliferate and retreat back into the B cell follicle, where they form GCs (Berek et al., 1991; Jacob et al., 1991; MacLennan, 1994; Rajewsky, 1996). Our experiments show that in the presence of an ongoing GC response, the initial response to a novel antigen proceeds by the canonical route of GC B cell development (i.e., by migration to the T/B interface) before reentering the B cell follicle. However, once the B cell has started to proliferate, it can choose to either initiate a new GC or join an existing GC that was formed in response to a heterologous antigen.

T cell help and GC reutilization

To determine whether GC B cell invasion is dependent on shared T cell help, we compared immunization with either Ars–chicken gamma globulin (CGG) or Ars-KLH in alum, followed by a boost with NP-CGG (lipopolysacharide free; Fig. 3 a). We found that when the same protein carrier was used for both immunization and boost, NP-specific B cells were found in the majority of all GCs (44 out of 61 GCs; Fig. 3, b [bottom] and c). The same results were observed when the double hapten conjugate NP,Ars-CGG was used in the boost after priming with Ars-CGG (Fig. S3, a–d); NP-specific B cells were found in almost every GC (12 out of 13 GCs; Fig. S3, c [bottom left] and d). Adding the adjuvant alum to the boost resulted in an increased invasion of GCs in both cases (21 out of 21 GCs; Fig. S3, c [bottom right] and d; and 36 out of 38 GCs; Fig. S4, a and b).

In contrast, at the same time point, there was no GC B cell formation and little invasion in the absence of preexisting T cell help. Immunization with Ars-KLH followed by injection with NP-CGG only produced a few mixed Ars- and NP-specific GCs (2 out of 98 GCs; Fig. 3, b [top] and c), whereas the rest was Ars specific. Similarly, when the double hapten-conjugated NP,Ars-CGG was used in the boost after priming with Ars-KLH (Fig. S3 a), NP-specific B cells were not found in GCs (0 out of 17 GCs; Fig. S3, c [top left] and d). Therefore, antibodies against a common epitope cannot be responsible for the effect. However, adding alum to the boost with NP-CGG or NP,Ars-CGG produced mixed GCs in both cases (6 out of 21 GCs; Fig. S3, c [top right] and d; and 34 out of 76; Fig. S4, a and b). Therefore, T cell help is required for B cells to join ongoing GCs.

We found delayed kinetics but highly efficient GC invasion when the protein carrier was switched but an adjuvant was provided in the boost. When mice were primed with Ars-KLH in alum and boosted with NP-OVA–containing LPS (Fig. 4 a), NP-specific B cells only appeared in heterologous Ars-specific GCs on day 6 (Fig. 4, b [bottom right] and c). All of the NP-specific GCs were mixed and also contained Ars-specific B cells (Fig. 4 c). In contrast, NP-specific B cells were already present in GCs in large numbers by day 4 when the carrier was shared (Fig. 4, b [top left] and c).

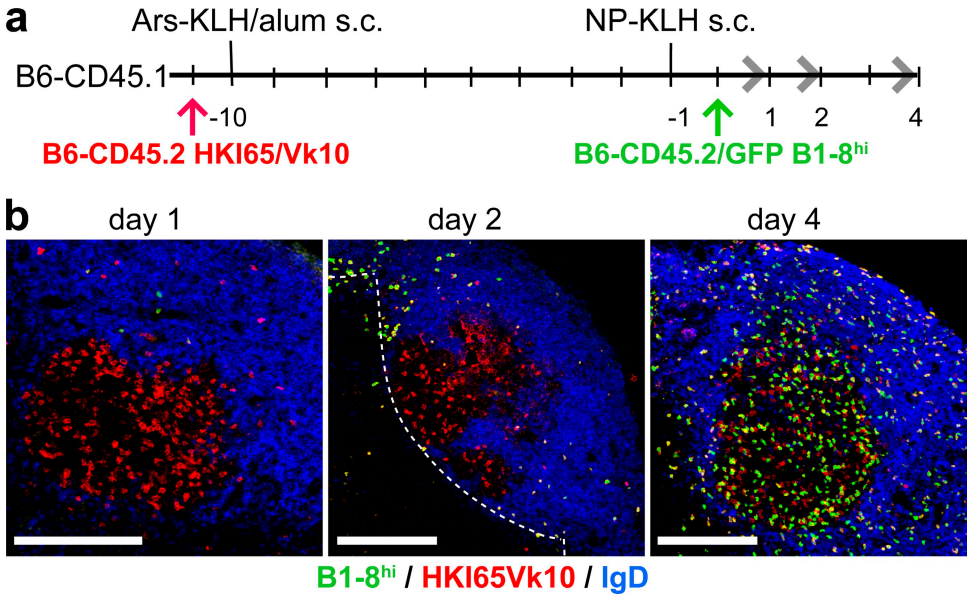

Figure 2. Kinetics of GC invasion. (a) Time line of immunization and B cell transfer. Ars-specific B cells (B6-CD45.2 HKI65/Vk10) were transferred into wild-type (B6-CD45.1) mice. 11 d later (day 0), NP-specific B cells (B6-CD45.2/GFP B1-8^{hi}) were transferred. Mice were immunized with Ars-KLH in alum 24 h after Ars-specific cells were transferred. 1 d before the transfer of NP-specific B cells, mice were boosted with NP-KLH. (b) Histological sections of lymph nodes harvested at 1, 2, and 4 d after NP-KLH boost stained with CD45.2 (red) and IgD (blue) to label all transferred B cells (HKI65/Vk10 and B1-8^{hi}) and naive B cells, respectively. Transferred NP-specific B1-8^{hi} B cells were additionally GFP^{+} (green). Representative images of secondary follicles from two independent experiments are displayed. The dashed line indicates the T/B cell interface. Bars, 200 µm.

We conclude that in the presence of T cell help, B cells rapidly enter preexisting GCs containing B cells that are specific for heterologous antigens. In the absence of shared T cell help, B cell invasion of established GCs still occurs; however, it occurs with delayed kinetics that are consistent with de novo development of helper T cells.

B cells' ability to join preexisting heterologous GCs would be an advantage in any infection that involves the development of variant pathogens, such as HIV, or parasites with variant coat proteins. In these types of infections, B cells specific for a nascent variant might be able to rapidly join a GC that already contained shared T cell help.

In contrast, this mechanism might, in part, facilitate the diversification of autoantibody responses during the course of autoimmune diseases, a phenomenon referred to as epitope spreading (Deshmukh et al., 2005). For example, in systemic lupus erythematosus, the first autoantibodies to be detected are frequently specific for SmD (Smith D). However, in later stages of the disease, affected individuals typically develop antibodies to A–ribonuclear protein (RNP) and/or SmB (Deshmukh et al., 2002). SmD, A-RNP and SmB are all part of the U1–small nuclear (sn) RNP complex; therefore, anti–A-RNP or –SmB-specific B cells would share cognate T cell help with anti-SmD B cells. Also, any GC-containing

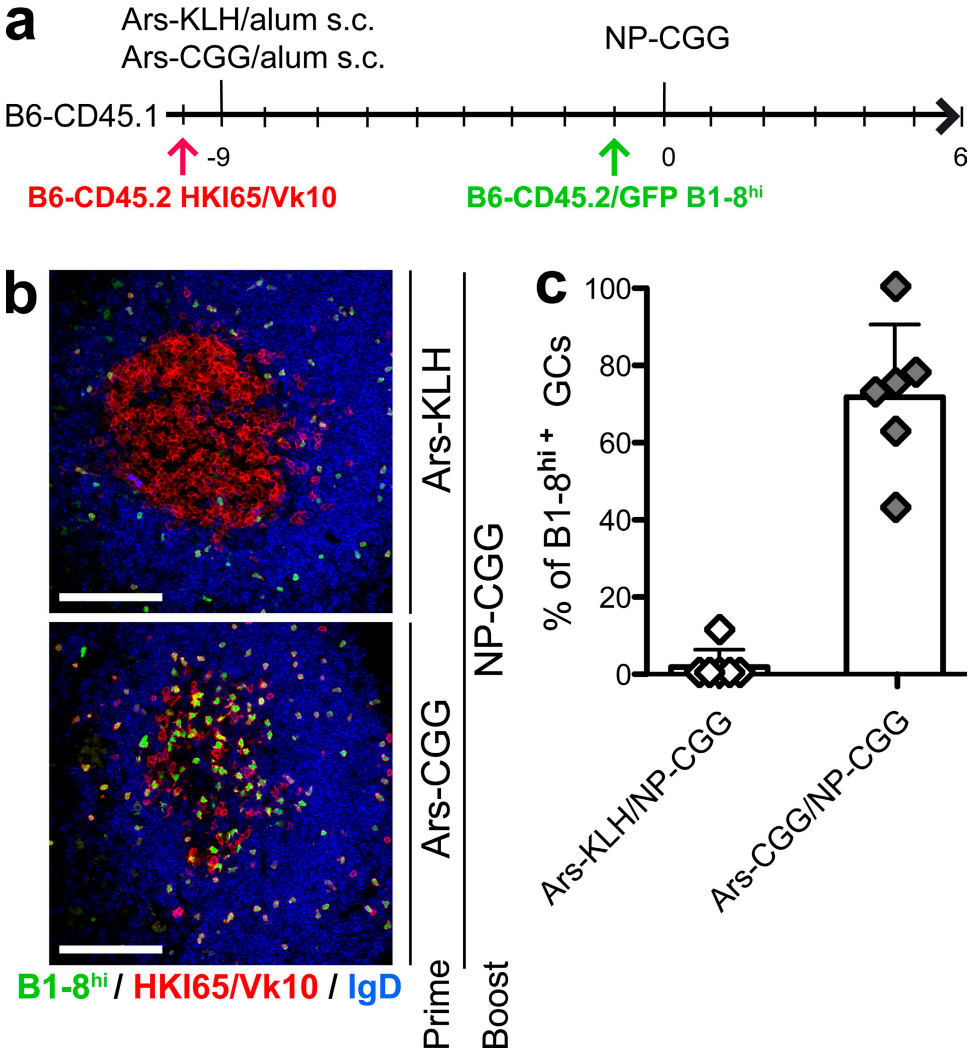

Figure 3. Invasion of heterogeneous GCs in the presence and absence of preexisting T cell help. (a) Time line of immunization and B cell transfer. Ars-specific B cells (B6-CD45.2 HKI65/Vk10) were transferred 1 d before primary immunization (day −10) and NP-specific B cells (B6-CD45.2/GFP B1-8^{hi}) were transferred 1 d before boosting (day −1) into wild-type (B6-CD45.1) mice. Mice were immunized with either Ars-KLH or Ars-CGG in alum. All mice were boosted with NP-CGG. (b) Representative histological sections of secondary follicles of lymph nodes harvested 6 d after NP-CGG boost stained with CD45.2 (red) and IgD (blue) to label all transferred B cells (HKI65/Vk10 and B1-8^{hi}) and naive B cells, respectively. Transferred NP-specific B1-8^{hi} B cells were additionally GFP^{+} (green). Antigens used for priming and boosting are indicated on the right. The top and bottom show data obtained from mice that were primed with Ars-KLH and Ars-CGG, respectively. All mice were boosted with NP-CGG. Bars, 100 µm. (c) Statistical analysis of data representatively shown in b. GCs were categorized into B1-8^{hi} positive and negative. Symbols represent the percentage of GCs containing B1-8^{hi} transferred B cells for each individual mouse. Error bars show the standard deviation. Two experiments were performed with a total of six mice per condition.

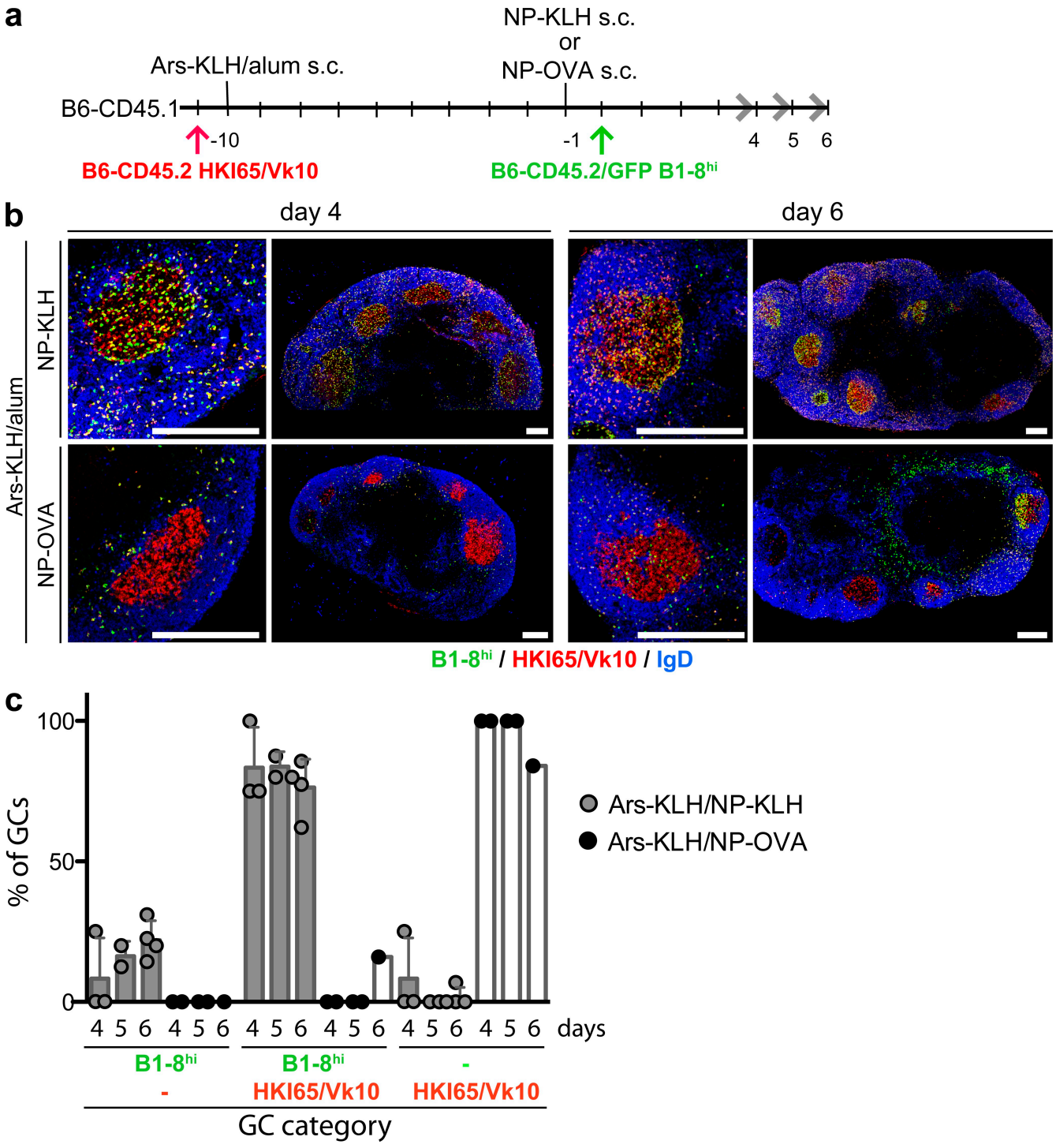

Figure 4. Delayed invasion in the absence of preexisting T cell help in GCs. (a) Time line of immunization and B cell transfer. Ars-specific B cells (B6-CD45.2 HKI65/Vk10) were transferred into wild-type (B6-CD45.1) mice. 11 d later (day 0), NP-specific B cells (B6-CD45.2/GFP B1-8^{hi}) were transferred. Mice were immunized with Ars-KLH in alum 1 d after Ars-specific cells were transferred. 1 d before the transfer of NP-specific B cells, mice were boosted with either NP-KLH or NP-OVA. (b) Histological sections of lymph nodes harvested 4 d (left four) and 6 d (right four) after NP-KLH (top) or NP-OVA (bottom) boost. Sections were stained with CD45.2 (red) and IgD (blue) to label all transferred B cells (HKI65/Vk10 and B1-8^{hi}) and naive B cells, respectively. Transferred NP-specific B1-8^{hi} B cells were additionally GFP^{+} (green). Bars, 200 µm. (c) Statistical analysis of data represented in b. GCs were categorized into the same three groups as described in Fig 1 c. Symbols indicate the percentage of GCs in one of the categories for each individual mouse. Error bars show the standard deviation. Two independent experiments were performed with a total of three or two mice.

SmD-reactive B cells would also contain anti–U1-snRNP-specific T cells and could be joined by activated anti–A-RNP or –SmB B cells during the course of the disease.

Two-photon imaging revealed that GCs are dynamic open structures. Naive B cells continually transit through the GC light zone, where they interact with antigen-bearing FDCs (Schwickert et al., 2007). If a B cell carries antigen in the form of immune complexes bound to complement receptors, the latter may be deposited on FDCs (Phan et al., 2007). Alternatively, if the naive cell is specific for the antigens displayed by the FDC, the interaction of the two cell types might lead to B cell activation and, ultimately, to GC invasion (Schwickert et al., 2007). These dynamic features are consistent with the observation that GCs contain multiple clones of unrelated cells, as well as naive B cells, and that the same clone of B cells can be found in more than one GC (Küppers et al., 1993; Bende et al., 2007). Together with these observations, our experiments suggest a new model for the GC, one which is open to naive B cell transit as well as to colonization by B cells responding to heterologous antigens.

MATERIALS AND METHODS

Mice. C57BL/6 (B6-CD45.2), B6-CD45.1, and B6-GFP (Schaefer et al., 2001) mice were purchased from The Jackson Laboratory. B1-8^{hi} (Shih et al., 2002) and HKI65/Vk10 (Heltemes-Harris et al., 2004; Liu et al., 2007) IgH knockin mice were maintained at the Rockefeller University and the Thomas Jefferson University. For adoptive transfer experiments, donor mice were 8–16 and recipients were 6–10 wk old. Mice were housed under specific pathogen-free conditions. All animal protocols were approved by the Rockefeller and the Thomas Jefferson University Animal Care and Use Committees.

Immunization. Mice were primed with 25–40 μg antigen precipitated in alum (2:1) injected s.c. into their hind footpads and into the base of the tail. 9–10 d later, they were boosted by injection with 50–80 μg of soluble or alum-precipitated antigen s.c. in their hind footpads and into the base of the tail.

Adoptive B cell transfer. B cells were purified by immunomagnetic depletion with anti–CD43-beads (Miltenyi Biotec). NP-specific B cells were further enriched by depletion of Igκ$^+$ cells (anti–Igκ-PE [BD] and anti-PE beads [Miltenyi Biotec]). 2–3 × 10^6 HKI65/Vk10 and B1-8^{hi} Igλ$^+$ B cells were transferred i.v. 1 d before or after the antigen boost.

Immunofluorescence. Cryostat sections of lymph nodes were fixed and stained as described previously (Lindquist et al., 2004). In brief, organs were fixed in PBS with 4% paraformaldehyde plus 10% sucrose and cryoprotected in PBS plus 30% sucrose before being embedded in optimum cutting temperature compound (OCT) and frozen. Frozen lymph nodes and spleens were sectioned (20 μm thickness) on a microtome and fixed in acetone. For immunostaining, all incubations were performed in a humidified chamber at room temperature. Sections were blocked in 5% BSA, 10% mouse serum, and sequentially with excess streptavidin and biotin (Vector Laboratories). The following antibodies were used for staining: anti–IgD-Alexa Fluor 647 (1:200; eBioscience), anti–IgD-FITC (1:100; eBioscience), anti–CD45.2-PE (1:250; eBioscience), PNA-biotin (1:1,000; Vector Laboratories), CD35-bio (1:500; eBioscience), and SA-Cy3 (1:500; Jackson ImmunoResearch Laboratories).

Laser microdissection. Lymph nodes were embedded in OCT, frozen, sectioned (20 μm thickness) on a microtome, and collected on membrane slides (Molecular Machines & Industries). Sections were fixed with 75% Ethanol for 30 s, washed with PBS for 2 min, incubated with anti–IgD-FITC in PBS for 5 min at 4°C, washed twice with PBS for 1 min, and dehydrated by incubating for 30 s in 75% ethanol followed by 95% ethanol. GCs (IgD$^-$ regions in B cell follicles) were laser dissected on a Cellcut system (Molecular Machines & Industries) fitted with a 355-nm solid-state laser at the Rockefeller Bio-imaging facility and collected in nuclease-free tubes with adhesive lids (Molecular Machines & Industries). Biopsies from the same GCs but from serial lymph node sections were collected and processed separately. The QIAamp DNA micro kit (QIAGEN) was used to isolate genomic DNA.

PCR and sequence analysis. Nested PCR was used to amplify V_H186.2-J_H2 and S107-J_H1 genes from GC B cells. NP-specific V_H186.2-J_H2 clones were amplified using the outer primers FO_58_V_H186.2 (5′-CATGGGATGGAGCTGTATCATGC-3′) and RO_55.9_J_H2 (5′-CTCACAAGAGTCCGATAGACCCTG-3′) and 25 cycles at 94°C for 30 s, 55.5°C for 30 s, and 72°C for 90 s, followed by the inner primers FI_55.7_V_H186.2 (5′-GGTGACAATGACATCCACTTTGC-3′) and RI_56_J_H2 (5′-GACTGTGAGAGTGGTGCCTTG-3′) and 25 cycles at 94°C for 30 s, 55.5°C for 30 s, and 72°C for 90 s. PC-specific S107-J_H1 clones were amplified using the outer primers FO_58.8_S107 (5′-CCTGAGTTCCCCAATCTTCACATTC-3′) and RO_59.1_J_H1 (5′-AGCCTCTGACTGCCTCTTTTCCTG-3′) and 25 cycles at 94°C for 30 s, 57°C for 30 s, and 72°C for 90 s, followed by the inner primers FI_56.6_S107 (5′-CAGGTATCCAGTGTGAGGTGAAGC-3′) and RI_58.2_J_H1 (5′-CGTTTCAGAATGGAATGTGCAGA-3′) and 25 cycles at 94°C for 30 s, 55.5°C for 30 s, and 72°C for 90 s. PCR was performed with DNA from 25 GCs per condition and at least three serial biopsies per GC. All amplified products were cloned (Topo Cloning kit; Invitrogen), sequenced, and analyzed using MegAlign (DNASTAR). Unique sequences from individual GCs were analyzed for mutated clones and existence of the same clone in multiple serial sections. HotStarTaq (QIAGEN) DNA polymerase with an error rate of ∼2 × 10^{-5}/nucleotide and cycle was preferred over high-fidelity enzymes with a 10× lower error rate because of its high amplification efficiency. The mutation frequency was ∼10^{-2}. The mutation frequency for PC-specific sequences was 0.8 × 10^{-2} or 1.1 × 10^{-2} for mice that were boosted with PC-KLH or NP-KLH, respectively, and for NP-specific sequences was 1.2 × 10^{-2} or 1.1 × 10^{-2} for mice that were boosted with PC-KLH or NP-KLH, respectively.

Confocal microscopy. Confocal images were acquired on an LSM 510 system (Carl Zeiss, Inc.) with a 488-, 543-, and 633-nm excitation line at the Rockefeller Bio-Imaging Facility. Z-stack (2–4 planes, 3-μm z-steps) images were obtained with a C-Apochromat 40× (NA 1.2, W corr), a Plan Apochromat 20× (NA 0.75), and a Plan Neofluar 10× (NA 0.3) objective. An array of 25 or 40× images was taken with a motorized stage to capture the entire cut surface of the lymph node.

Analysis of GC composition in histological sections. GCs, defined by PNA$^+$, CD35$^+$, or IgD$^-$ staining in B cell follicles, were categorized according to their composition. GCs enriched in both transferred Ars- and NP-specific B cell populations were classified as mixed. GCs were only scored as positive for the transferred B cell type if we found a higher density and IgD$^-$ of transferred cells in the GC than in the B cell follicle.

Online supplemental material. Fig. S1 and Fig. S2 show the invasion of preexisting GCs in wild-type mice by laser microdissection and BCR sequence analysis. Fig. S3 demonstrates that invasion of heterogeneous GCs in the presence of antigen-specific antibodies is depended on the availability of T cell help. Fig. S4 shows that invasion of heterogeneous GCs depends on the activation of antigen-specific T cell help. Online supplemental material is available at http://www.jem.org/cgi/content/full/jem.20091225/DC1.

We thank S. Fenn and G. Victora for technical assistance, S. Davis for helpful comments on the manuscript, and all members of the Nussenzweig laboratory for their suggestions.

This work was supported by the Schering Foundation (T.A. Schwickert), National Institutes of Health (grants 1R0AI072529-01 and 5R01AI037526 to M.C. Nussenzweig), and Howard Hughes Medical Institute (M.C. Nussenzweig).

The authors have no conflicting financial interests.

Submitted: 4 June 2009
Accepted: 29 October 2009

REFERENCES

Allen, C.D., T. Okada, H.L. Tang, and J.G. Cyster. 2007. Imaging of germinal center selection events during affinity maturation. *Science*. 315:528–531. doi:10.1126/science.1136736

Ansel, K.M., L.J. McHeyzer-Williams, V.N. Ngo, M.G. McHeyzer-Williams, and J.G. Cyster. 1999. In vivo–activated CD4 T cells upregulate CXC chemokine receptor 5 and reprogram their response to lymphoid chemokines. *J. Exp. Med.* 190:1123–1134. doi:10.1084/jem.190.8.1123

Bachmann, M.F., B. Odermatt, H. Hengartner, and R.M. Zinkernagel. 1996. Induction of long-lived germinal centers associated with persisting antigen after viral infection. *J. Exp. Med.* 183:2259–2269. doi:10.1084/jem.183.5.2259

Bende, R.J., F. van Maldegem, M. Triesscheijn, T.A. Wormhoudt, R. Guijt, and C.J. van Noesel. 2007. Germinal centers in human lymph nodes contain reactivated memory B cells. *J. Exp. Med.* 204:2655–2665. doi:10.1084/jem.20071006

Berek, C., A. Berger, and M. Apel. 1991. Maturation of the immune response in germinal centers. *Cell.* 67:1121–1129. doi:10.1016/0092-8674(91)90289-B

Carrasco, Y.R., and F.D. Batista. 2007. B cells acquire particulate antigen in a macrophage-rich area at the boundary between the follicle and the subcapsular sinus of the lymph node. *Immunity*. 27:160–171. doi:10.1016/j.immuni.2007.06.007

Casola, S., K.L. Otipoby, M. Alimzhanov, S. Humme, N. Uyttersprot, J.L. Kutok, M.C. Carroll, and K. Rajewsky. 2004. B cell receptor signal strength determines B cell fate. *Nat. Immunol.* 5:317–327. doi:10.1038/ni1036

Coffey, F., B. Alabyev, and T. Manser. 2009. Initial clonal expansion of germinal center B cells takes place at the perimeter of follicles. *Immunity*. 30:599–609. doi:10.1016/j.immuni.2009.01.011

Deshmukh, U.S., C.C. Kannapell, and S.M. Fu. 2002. Immune responses to small nuclear ribonucleoproteins: antigen-dependent distinct B cell epitope spreading patterns in mice immunized with recombinant polypeptides of small nuclear ribonucleoproteins. *J. Immunol.* 168:5326–5332.

Deshmukh, U.S., H. Bagavant, J. Lewis, F. Gaskin, and S.M. Fu. 2005. Epitope spreading within lupus-associated ribonucleoprotein antigens. *Clin. Immunol.* 117:112–120. doi:10.1016/j.clim.2005.07.002

Figge, M.T., A. Garin, M. Gunzer, M. Kosco-Vilbois, K.M. Toellner, and M. Meyer-Hermann. 2008. Deriving a germinal center lymphocyte migration model from two-photon data. *J. Exp. Med.* 205:3019–3029. doi:10.1084/jem.20081160

Hauser, A.E., T. Junt, T.R. Mempel, M.W. Sneddon, S.H. Kleinstein, S.E. Henrickson, U.H. von Andrian, M.J. Shlomchik, and A.M. Haberman. 2007. Definition of germinal-center B cell migration in vivo reveals predominant intrazonal circulation patterns. *Immunity*. 26:655–667. doi:10.1016/j.immuni.2007.04.008

Heltemes-Harris, L., X. Liu, and T. Manser. 2004. Progressive surface B cell antigen receptor down-regulation accompanies efficient development of antinuclear antigen B cells to mature, follicular phenotype. *J. Immunol.* 172:823–833.

Jacob, J., G. Kelsoe, K. Rajewsky, and U. Weiss. 1991. Intraclonal generation of antibody mutants in germinal centres. *Nature*. 354:389–392. doi:10.1038/354389a0

Junt, T., E.A. Moseman, M. Iannacone, S. Massberg, P.A. Lang, M. Boes, K. Fink, S.E. Henrickson, D.M. Shayakhmetov, N.C. Di Paolo, et al. 2007. Subcapsular sinus macrophages in lymph nodes clear lymph-borne viruses and present them to antiviral B cells. *Nature*. 450:110–114. doi:10.1038/nature06287

Kroese, F.G., A.S. Wubbena, H.G. Seijen, and P. Nieuwenhuis. 1987. Germinal centers develop oligoclonally. *Eur. J. Immunol.* 17:1069–1072. doi:10.1002/eji.1830170726

Küppers, R., M. Zhao, M.L. Hansmann, and K. Rajewsky. 1993. Tracing B cell development in human germinal centres by molecular analysis of single cells picked from histological sections. *EMBO J.* 12:4955–4967.

Lindquist, R.L., G. Shakhar, D. Dudziak, H. Wardemann, T. Eisenreich, M.L. Dustin, and M.C. Nussenzweig. 2004. Visualizing dendritic cell networks in vivo. *Nat. Immunol.* 5:1243–1250. doi:10.1038/ni1139

Liu, Y.J., J. Zhang, P.J. Lane, E.Y. Chan, and I.C. MacLennan. 1991. Sites of specific B cell activation in primary and secondary responses to T cell-dependent and T cell-independent antigens. *Eur. J. Immunol.* 21:2951–2962. doi:10.1002/eji.1830211209

Liu, X., L.J. Wysocki, and T. Manser. 2007. Autoantigen-B cell antigen receptor interactions that regulate expression of B cell antigen receptor Loci. *J. Immunol.* 178:5035–5047.

MacLennan, I.C. 1994. Germinal centers. *Annu. Rev. Immunol.* 12:117–139. doi:10.1146/annurev.iy.12.040194.001001

Okada, T., and J.G. Cyster. 2006. B cell migration and interactions in the early phase of antibody responses. *Curr. Opin. Immunol.* 18:278–285. doi:10.1016/j.coi.2006.02.005

Okada, T., M.J. Miller, I. Parker, M.F. Krummel, M. Neighbors, S.B. Hartley, A. O'Garra, M.D. Cahalan, and J.G. Cyster. 2005. Antigen-engaged B cells undergo chemotaxis toward the T zone and form motile conjugates with helper T cells. *PLoS Biol.* 3:e150. doi:10.1371/journal.pbio.0030150

Phan, T.G., I. Grigorova, T. Okada, and J.G. Cyster. 2007. Subcapsular encounter and complement-dependent transport of immune complexes by lymph node B cells. *Nat. Immunol.* 8:992–1000. doi:10.1038/ni1494

Rajewsky, K. 1996. Clonal selection and learning in the antibody system. *Nature*. 381:751–758. doi:10.1038/381751a0

Reth, M., G.J. Hämmerling, and K. Rajewsky. 1978. Analysis of the repertoire of anti-NP antibodies in C57BL/6 mice by cell fusion. I. Characterization of antibody families in the primary and hyperimmune response. *Eur. J. Immunol.* 8:393–400. doi:10.1002/eji.1830080605

Roozendaal, R., T.R. Mempel, L.A. Pitcher, S.F. Gonzalez, A. Verschoor, R.E. Mebius, U.H. von Andrian, and M.C. Carroll. 2009. Conduits mediate transport of low-molecular-weight antigen to lymph node follicles. *Immunity*. 30:264–276. doi:10.1016/j.immuni.2008.12.014

Rudikoff, S., and M. Potter. 1980. Allelic forms of the immunoglobulin heavy chain variable region. *J. Immunol.* 124:2089–2092.

Ruppert, V.J., K. Williams, and J.L. Claflin. 1980. Specific clonal regulation in the response to phosphocholine. I. Genetic analysis of the response of a distinct idiotype (M511 Id). *J. Immunol.* 124:1068–1074.

Schaefer, B.C., M.L. Schaefer, J.W. Kappler, P. Marrack, and R.M. Kedl. 2001. Observation of antigen-dependent CD8+ T-cell/dendritic cell interactions in vivo. *Cell. Immunol.* 214:110–122. doi:10.1006/cimm.2001.1895

Schwickert, T.A., R.L. Lindquist, G. Shakhar, G. Livshits, D. Skokos, M.H. Kosco-Vilbois, M.L. Dustin, and M.C. Nussenzweig. 2007. In vivo imaging of germinal centres reveals a dynamic open structure. *Nature*. 446:83–87. doi:10.1038/nature05573

Shih, T.A., M. Roederer, and M.C. Nussenzweig. 2002. Role of antigen receptor affinity in T cell-independent antibody responses in vivo. *Nat. Immunol.* 3:399–406. doi:10.1038/ni776

Suzuki, K., I. Grigorova, T.G. Phan, L.M. Kelly, and J.G. Cyster. 2009. Visualizing B cell capture of cognate antigen from follicular dendritic cells. *J. Exp. Med.* 206:1485–1493. doi:10.1084/jem.20090209